Chinese Journal of
POLYMER SCIENCE

ARTICLE

https://doi.org/10.1007/s10118-020-2448-0
Chinese J. Polym. Sci. **2020**, *38*, 1409–1417

Diffusion of a Ring Threaded on a Linear Chain

Zhen-Hua Wang[a,b], Yu-Yuan Lu[a*], Hui Jin[c], Chuan-Fu Luo[a,b], and Li-Jia An[a,b]

[a] *State Key Laboratory of Polymer Physics and Chemistry, Changchun Institute of Applied Chemistry, Chinese Academy of Sciences, Changchun 130022, China*
[b] *University of Science and Technology of China, Hefei 230026, China*
[c] *Changchun Institute of Optics, Fine Mechanics and Physics, Chinese Academy of Sciences, Changchun 130033, China*

Abstract A mesoscopic simulation is applied to investigate the effects of hydrodynamic interactions and axial chains on the dynamics of threaded rings. The hydrodynamic interactions significantly speed up the diffusion and relaxation of both free and threaded rings. The decoupled diffusion and relaxation dynamics indicate the broken of the Einstein-Stokes relationship. The diffusion of a ring threaded on a flexible chain exhibits a synergism effect compared to that on an axial rod, which originates from the self-diffusion of the ring and the reptation-like motion of the axial chain. Meanwhile, hydrodynamic interactions significantly improve the synergism effect, leading to an enhanced sliding motion of the threaded ring. The faster sliding of threaded rings suggests that the entropic barrier is negligible, which agrees well with the basic assumption of barrier-less confining tube at equilibrium in tube theory. Our results provide a new perspective on analysis of the effects of topology constraints on polymer dynamics.

Keywords Hydrodynamic interactions; Threaded ring; Sliding dynamics; Diffusion and relaxation

Citation: Wang, Z. H.; Lu, Y. Y.; Jin, H.; Luo, C. F.; An, L. J. Diffusion of a ring threaded on a linear chain. *Chinese J. Polym. Sci.* **2020**, *38*, 1409–1417.

INTRODUCTION

Understanding the effects of molecular topologies and entanglements on the static, dynamic, and rheological properties of polymer solutions or melts remains a challenging problem in polymer physics.[1] Compared with linear chains, the absence of free ends for ring polymers generally leads to lower zero-shear viscosity[2,3] and higher recoverable compliance.[4] Meanwhile, many dynamic processes requiring free chain ends do not exist in ring polymer melts, such as reptation motion and constraint release.[1] Therefore, linear and ring polymer chains are widely used to deal with the complex inter-chain interactions,[5–10] being considered as two fundamental chain models in polymer physics.

A simple combination of linear and ring chains brings about large changes of rheological properties for polymer fluids. For example, even a small fraction of linear contaminants leads to a drastic increase in viscosity.[3,11] A complete understanding of mixed (ring-linear) chain topology blends is of fundamental interest to polymer physics. To interpret the diffusion mechanism of a ring polymer along a threaded linear chain, the threaded-ring model was proposed.[5] A particular threaded-ring structure is depicted in Fig. 1, where a ring polymer is threaded on a linear chain. Such threaded-ring structure is successfully applied to realize the structure transformations between polymers with different topologies,[12–14] and to represent the entanglements or slip-links in polymer physics.[15–20] In addition to theoretical applications, such threaded-ring structure also plays an essential role in molecular design. For example, rotaxane is a typical topologically interlocked molecule which has a similar threaded-ring structure, with both ends of the axial molecule being connected to bulky groups that prevent unthreading of the ring.[21–26] The weak non-covalent interactions between the linear and ring components lead to unique dynamic properties,[27] making the threaded-ring structure a versatile platform to develop various artificial molecular machines,[28–32] such as molecular shuttles,[33–35] molecular switches,[36–38] and molecular muscles.[39] Therefore, the threaded-ring structure has attracted growing concerns in polymer physics and material science. A great number of studies have been devoted to this promising subject.[5,15–17,19,20,40–45]

de Gennes[40] proposed a simple model to analyze theoretically the sliding motion of a ring in sliding gels and found that a rather weak force is enough to drive the ring to slide. However, the oversimplified model fails to account for the softness of sliding gels with movable cross-links. Compared with traditional chemical and physical gels, the threaded-ring structure in sliding gels greatly affected their mechanical properties. Lee *et al.*[46,47] pointed out that the threading between the rings is the main reason for slowing down of ring polymer diffusion in melts. Schroeder *et al.*[48] directly observed the non-equilibrium dynamics of rings in the background solution of linear chains under extensional flows, by using single molecule fluorescence microscopy. They found that large conformational fluctuations of ring polymers occur even long after the initial transient stretching process, and the fluctuations can be attributed to the threading events

* Corresponding author, E-mail: yylu@ciac.ac.cn

Received March 14, 2020; Accepted April 27, 2020; Published online June 30, 2020

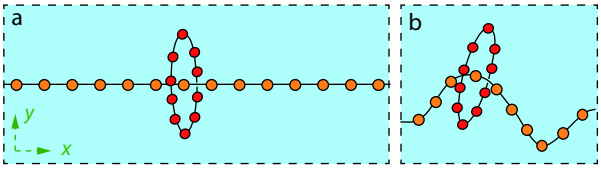

Fig. 1 Schematic illustration of threaded-ring structures, with a semiflexible ring threaded on (a) a rod-like polymer chain and (b) a flexible linear polymer chain.

between ring and linear chains.

Recently, Ito *et al.*[49] succeeded in synthesizing polyrotaxane (several rings in the rotaxane structure) molecules consisting of α-cyclodextrins (CDs) as rings and poly(ethylene glycol) (PEG) as axial chains. They designed and developed a series of soft materials with unique mechanical properties[50–53] by cross-linking the ring molecules in the cyclodextrin-based polyrotaxanes, such as the pulley effect[54] and large crack resistance.[55,56] The novel polymeric materials are referred to as "slide-ring gels" by the developers, named from the freely sliding motions of rings on the molecular level. To further understand the novel properties of slide-ring gels and corresponding mechanisms, Ito *et al.*[57,58] also investigated the diffusion dynamics of ring molecule in the rotaxane structure. They quantified the sliding motion of CDs along a PEG polymer chain for the first time by using the full-atomistic molecular dynamics.[57] They proposed a simple model to clarify the retardation of the sliding motion of CD along PEG *via* combing the Einstein-Stokes diffusion equation and the Arrhenius equation, which is caused by the energy barrier between CD and PEG. Ito *et al.*[58] also performed a series of Langevin simulations to investigate the sliding dynamics of a rigid ring threaded on different axial polymers. They found that the rigid ring on a coil-like chain slides faster than that on a fixed rod due to the reptation-like chain motion. Their results indicate that the sliding dynamics of a rigid ring is dominated by the coupling effect between the ring diffusion and the fluctuating behaviors of the axial polymers. However, the effects of hydrodynamic interactions on the ring dynamics are not considered in these studies.

Hydrodynamic interactions have a dramatic effect on polymer dynamics.[1,59] In simulations, inclusion of hydrodynamic interactions can accelerate polymer-collapse dynamics,[60,61] speed up ejection from capsid,[62] and lead to the non-monotonic increase of polymer size under a shear flow.[63–67] However, the effect of hydrodynamic interactions on the diffusion of ring molecule in a threaded-ring structure is still unknown. The coupling effect between conformations and flow fields directly results in complex behaviors of a ring molecule treaded on a linear chain. Therefore, further investigations of the effects of hydrodynamic interactions on the dynamics of a threaded-ring structure not only are of great importance to the theory and practice but also provide new insights into the structure-property relationship of topological gels based on the threaded-ring supramolecular complexes.

In this work, a hybrid simulation method (multi-particle collision dynamics[68,69] coupled with molecular dynamics, MPCD+MD) is applied to investigate the effects of hydrodynamic interactions on the dynamics of rigid ring in the threaded-ring model. We elucidate the different diffusion behaviors of rings threaded on between rigid and flexible axial polymer chains. We further systematically evaluate the influence of hydrodynamic interactions on the ring dynamics. The rest of this paper is organized as follows. In the following section, we describe the simulation method and polymer models in detail. Subsequently, results and discussion are provided accordingly. At last, we briefly summarize the main conclusions of this work and present our outlook for future simulations.

MODEL AND SIMULATION METHOD

Solvent Model

The MPCD algorithm[68,69] includes two steps: the streaming step and the collision step. In the streaming step, each solvent particle moves according to the following equation:

$$\mathbf{r}_i(t+h) = \mathbf{r}_i(t) + \mathbf{v}_i(t)h \tag{1}$$

where, $\mathbf{r}_i$ and $\mathbf{v}_i$ are the position and velocity vectors of the i^{th} particle, respectively. h is the time interval in the MPCD simulation. In the following collision step, all solvent particles are sorted into cubic cells first, and then the velocities are updated *via*

$$\mathbf{v}_i(t+h) = \mathbf{v}_{\text{cm}}(t) + \mathbf{R}(\alpha)\left[\mathbf{v}_i(t) - \mathbf{v}_{\text{cm}}(t)\right] \tag{2}$$

where $\mathbf{v}_{\text{cm}}$ is the center-of-mass velocity of the cell including the i^{th} particle,

$$\mathbf{v}_{\text{cm}} = \frac{\sum\limits_{i\in\text{cell}} m\mathbf{v}_i}{\sum\limits_{i\in\text{cell}} m} = \frac{\sum\limits_{i\in\text{cell}} \mathbf{v}_i}{N_{\text{cell}}} \tag{3}$$

with N_{cell} being the number of solvent particles in a cell. $\mathbf{R}(\alpha)$ is a rotation matrix, which is used to rotate $[\mathbf{v}_i(t) - \mathbf{v}_{\text{cm}}(t)]$ around a randomly chosen axis with the fixed angle α. A random shift was introduced before each collision step to guarantee the Galilean invariance.[70] In other words, all particles are shifted by a translation vector whose components are chosen from a uniform distribution on the interval $[-a/2, a/2]$. Here, a is the side length of each cell. After the collision step, the particles are placed back to their original positions. In each cubic cell, the mass, momentum, and energy are conserved.

Polymer Model

The polymer chain is treated as a sequence of monomers interacting with each other *via* a truncated and shifted Lennard-Jones (LJ) potential[71] defined as

$$U_{\text{LJ}}(r_{ij}) = \begin{cases} 4\varepsilon\left[\left(\dfrac{\sigma}{r_{ij}}\right)^{12} - \left(\dfrac{\sigma}{r_{ij}}\right)^{6} + \dfrac{1}{4}\right]; & r_{ij} \leqslant \sqrt[6]{2}\sigma \\ 0 \qquad\qquad\qquad\qquad\quad ; & r_{ij} > \sqrt[6]{2}\sigma \end{cases} \tag{4}$$

where r_{ij} is the distance between the monomers i and j. ε and σ are the reduced energy and length units, respectively. For the consecutive monomers, a finitely extensible nonlinear elastic (FENE) potential[72] is applied by

$$U_{\text{FENE}}(r_{ij}) = \begin{cases} -\dfrac{1}{2}kr_{\text{bond}}^2 \ln\left[1 - \left(\dfrac{r_{ij}}{r_{\text{bond}}}\right)^2\right]; & r_{ij} \leqslant r_{\text{bond}} \\ \infty \qquad\qquad\qquad\qquad\quad ; & r_{ij} > r_{\text{bond}} \end{cases} \tag{5}$$

where $k = 30\varepsilon/\sigma^2$ and $r_{\text{bond}} = 1.5\sigma$.[71] In addition, the flexibility of polymer chain can be tuned by the bond bend potential, which is given by

$$U_{\text{BEND}}(\theta) = k_{\theta\text{ring}}(1 + \cos\theta) \tag{6}$$

https://doi.org/10.1007/s10118-020-2448-0

where $k_{\theta ring}$ is the bending constant of the angle between two neighboring bonds of ring polymer chains. $k_{\theta ring}$ is set to be 10ε, corresponding to a persistence length of about 9.09σ. Such parameter is appropriate to maintain the ring rigidity and to avoid excessive bond bend energy. The bonded monomers thus interact *via* sum of the three potentials, $U(r_{ij}) = U_{LJ}(r_{ij}) + U_{FENE}(r_{ij}) + U_{BEND}(\theta)$.

There are three different kinds of polymer models in this work: ring, rod, and flexible polymer chains. The ring polymer is threaded on an axial polymer, where the threading axle can be a rod-like or flexible chain. During the simulation, positions of all monomers in the rod chain keep unchanged, while for flexible axial chain, as a comparison, monomers are free to move, resulting in significant conformational fluctuations of the axial polymer.

The time evolution of the polymer monomers is calculated by the velocity Verlet algorithm:[73]

$$\begin{aligned} \mathbf{r}_j(t+\delta t) &= \mathbf{r}_j(t) + \mathbf{v}_j(t)\delta t + \frac{1}{2}\frac{\mathbf{f}_j(t)}{M}\delta t^2 \\ \mathbf{v}_j(t+\delta t) &= \mathbf{v}_j(t) + \frac{1}{2}\left[\frac{\mathbf{f}_j(t) + \mathbf{f}_j(t+\delta t)}{M}\right]\delta t \end{aligned} \tag{7}$$

where $\mathbf{r}_j$, $\mathbf{v}_j$, and $\mathbf{f}_j$ are the position, velocity, and force vectors of monomer j, respectively. M is the mass of monomer and δt denotes the time interval of the velocity Verlet algorithm.

In our simulations, ε, σ, and the mass of solvent particle m are set to be unity. Therefore, the unit of time is given by $(m\sigma^2/\varepsilon)^{1/2} = 1$. δt is chosen to be 0.0005 and the temperature of the system is kept at $k_BT = 1$.

MPCD+MD Hybrid Method

The solvent dynamics described above should be modified if a polymer chain is taken into account. The hydrodynamic interactions between a polymer and solvents are introduced in the collision steps.[74] Meanwhile, $\mathbf{v}_{cm}$ in the collision step is revised as:

$$\mathbf{v}_{cm} = \frac{\sum\limits_{i\in cell} m\mathbf{v}_{s,i} + \sum\limits_{i\in cell} M\mathbf{v}_{p,j}}{\sum\limits_{i\in cell} m + \sum\limits_{i\in cell} M} \tag{8}$$

with $\mathbf{v}_{s,i}$ and $\mathbf{v}_{p,j}$ being the velocity vectors of the solvent particle and the polymer monomer, respectively.

The side length of each cubic cell, a, is equal to σ. The average number density of solvent particles per cell ρ is chosen to be 10 and the mass of polymer bead is set as $M = \rho m = 10$. The rotation angle α is chosen to be 130°[75–77] and the time increment is set as $h = 0.1$. The data reported are average results over 100 independent runs.

Simulation Systems

In our simulations, the threaded-ring size can be changed easily by varying the number of ring monomers, N ($5 \le N \le 30$). Monomers of ring and axial polymer chains interact with each other *via* the non-bonded LJ potential, *i.e.*, Eq. (4).

The dimensions of the simulation box for Ring-on-Rod system (Fig. 1a) are set as $60a \times 20a \times 20a$ ($N \le 20$), $60a \times 23a \times 23a$ ($N = 24$), and $60a \times 30a \times 30a$ ($N = 30$). The rod chain is fixed in the simulation box and the chain ends are connected through the periodic boundary conditions (PBC) to avoid dethreading of the ring from the axial chain. For Ring-on-Chain system (Fig. 1b), the axial chain is a flexible linear polymer and the dimension of the simulation box is set to be $19a \times 30a \times 30a$. The axial rod or linear chain is aligned along the x-axis, as shown in Fig. 1.

Analysis of Size and Dynamics Properties

The polymer size is characterized by the mean-square radius of gyration, which is defined by

$$\left\langle R_g^2 \right\rangle^{1/2} = \left\langle \frac{1}{N}\sum_i^N (\mathbf{r}_i - \mathbf{r}_{cm})^2 \right\rangle; \quad \mathbf{r}_{cm} = \frac{1}{N}\sum_i^N \mathbf{r}_i \tag{9}$$

where $\langle \ldots \rangle$ indicates the ensemble average over all available conformations of polymer chains. The center-of-mass mean-square displacement (MSD) of polymer chains is given by

$$\text{MSD} = \left\langle (\mathbf{r}_{cm}(t) - \mathbf{r}_{cm}(0))^2 \right\rangle \tag{10}$$

which is calculated based on the Cartesian coordinates. To characterize the sliding diffusion, the relative MSD along the axial chain (r-MSD) is defined as

$$\text{r-MSD} = b^2 \left\langle (\text{ID}(t) - \text{ID}(0))^2 \right\rangle \tag{11}$$

where b is the average bond length and ID(t) represents the index number of axial chain which is closest to the center-of-mass of the ring molecule.

The above definitions of MSD and r-MSD are based on the three- and one- dimensional diffusions, respectively. Therefore, the corresponding diffusion coefficients (D for MSD, and D_{slide} for r-MSD) are calculated *via*

$$D = \frac{\Delta(\text{MSD})}{6\Delta t}; \quad D_{slide} = \frac{\Delta(\text{r-MSD})}{2\Delta t} \quad (\Delta t \gg 1\tau) \tag{12}$$

For comparison, the diffusion coefficients of free ring polymers with different chain sizes under PBC (D_0) are also calculated.

The relaxation dynamics for ring polymers is measured by the normalized autocorrelation function of diameter vector, $C(t)$. The function is defined as follows:

$$C(t) = \frac{\langle \boldsymbol{R}_d(t)\boldsymbol{R}_d(0)\rangle}{\langle \boldsymbol{R}_d^2(0)\rangle} \propto \exp\left(-\frac{t}{\tau_R}\right) \tag{13}$$

where $\boldsymbol{R}_d$ is the diameter vector that connects pair monomers separated by $N/2$ monomers. τ_R is the relaxation time of a ring polymer under PBC, which is extracted from the autocorrelation function, $C(t)$.

RESULTS AND DISCUSSION

Free Ring in Free Space

We first discuss the static and dynamical properties of free rings under periodic boundary conditions (3D PBC). As shown in Fig. 2(a), with the increase of bending constant k_θ, the ring size increases at first and then approaches the saturation value ($k_{\theta ring} > 50$), where the ring conformation is nearly a circle and its radius is about $Nb/(2\pi)$. The size of polymer ring with different monomers is plotted in Fig. 2(b). For both flexible ($k_{\theta ring} = 0$) and semiflexible ($k_{\theta ring} = 10$) polymer rings, the equilibrium sizes are hardly affected by hydrodynamic interactions. The introduction of bond bend energy leads to significant increase in ring size. For small semiflexible rings ($N \le 10$), the polymer size agrees well with the theoretical radius of the regular circle, while for large rings ($N > 10$), the size displays noticeable deviation from

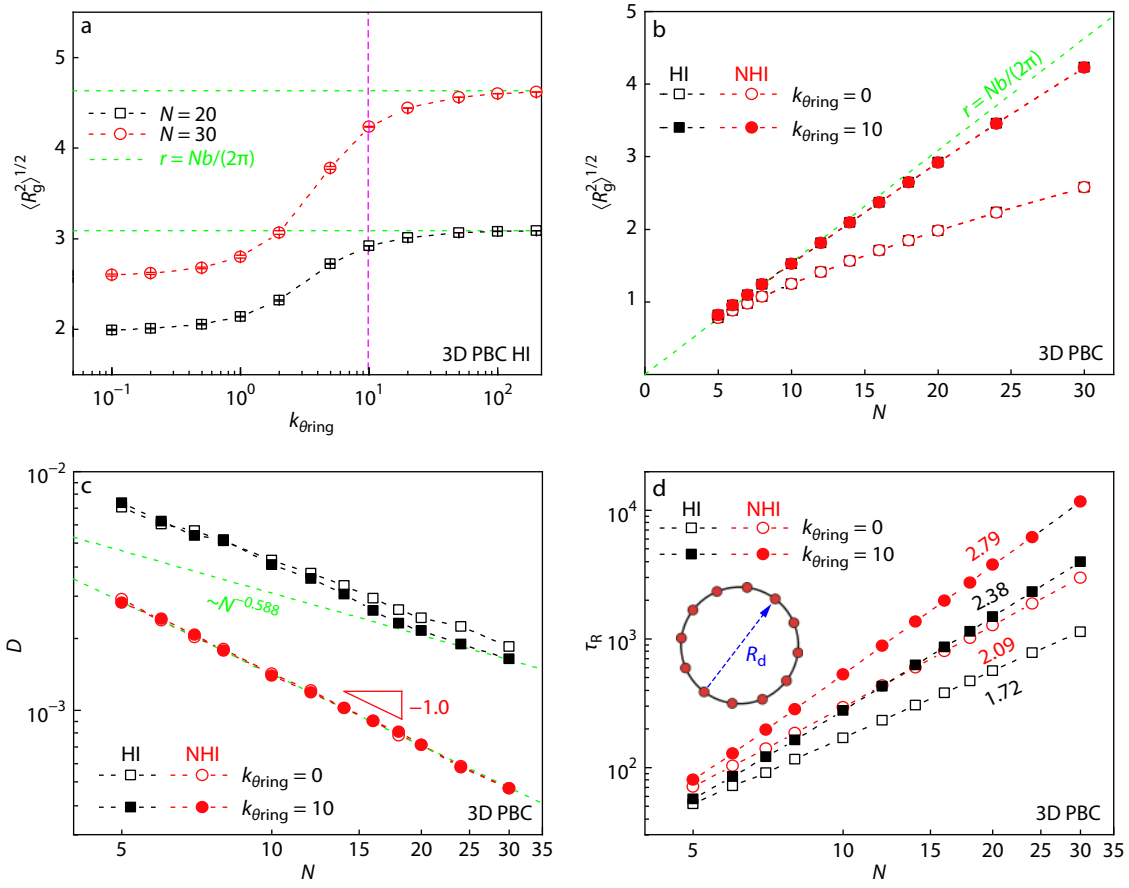

Fig. 2 The size and dynamics properties of free ring polymers with (HI) and without (NHI) hydrodynamic interactions under periodic boundary conditions. (a) The effect of bending constant of the bond angle $k_{\theta ring}$ on ring polymer size. (b) Polymer size with different numbers of monomers N in the ring chain with $k_{\theta ring}$ = 0, 10. (c) Diffusion and (d) relaxation of flexible/semiflexible ring polymers under periodic boundary conditions.

theoretical line.

According to the predictions of the Rouse and Zimm models, diffusion and relaxation of linear and ring polymers satisfy the following scaling relationships:

$$D_{Rouse} \propto N^{-1}, \quad D_{Zimm} \propto N^{-\nu} \propto N^{-0.588}$$
$$\tau_{Rouse} \propto N^{2}, \quad \tau_{Zimm} \propto N^{3\nu} \propto N^{1.76} \qquad (14)$$

As shown in Fig. 2(c), hydrodynamic interactions significantly speed up the diffusion of both flexible and semiflexible rings. For systems without hydrodynamic interactions (NHI), the diffusion coefficient scales inversely with chain length for rings with different flexibilities ($D \sim N^{-1}$), which is consistent with theoretical prediction of the Rouse model. The diffusion coefficients for flexible and semiflexible rings exhibit obvious difference as the chain length increases, if the hydrodynamic interactions (HI) are taken into account. The flexible ring diffuses a little faster due to its compact conformation and stronger hydrodynamic interactions between monomers. The diffusion scaling is valid only for large rings, because the hydrodynamic interactions are closely related with the monomer density. The hydrodynamic interactions also accelerate the relaxation behavior of polymer rings (Fig. 2d). On the contrary, chain rigidity greatly slows down the relaxation. For flexible rings with and without hydrodynamic interactions, the relaxation dynamics are in accord with the Zimm and Rouse scaling relationships, respectively. The scaling indexes for HI and NHI are significantly increased by the chain rigidity, indicating that the relaxation of semiflexible rings is hindered by extended conformations.

Threaded Ring on Fixed Rod

Before considering the general form of the threaded-ring structure, we started with a particularly simple version, where the ring polymer chain is threaded on a fixed rod (Ring-on-Rod). As shown in Fig. 3(a), the time evolutions of MSD for HI and NHI have similar curve shapes, but the value of MSD for HI is greater than that for NHI, suggesting that hydrodynamic interactions significantly improve the motion of threaded ring. For the smallest ring (N = 5, data not shown), the corresponding MSD keeps unchanged for either HI or NHI during the whole simulation, and the ring seems to be "frozen". Here, the "frozen" state implies strong interactions between the ring and axial chains, which is caused by the nonbonding potential between monomers of the two components. For ring chains with N = 6, although MSD scales linearly with time at long time scales, the maximum value of MSD approximately equals 3, which means that the diffusion ability of such a ring is extremely limited. Based on the x- and y- components of MSD (Figs. 3b and 3c) for the ring with N = 6, it is clear that the axial diffusion contributes exclusively to the ring motion. Moreover, for small

https://doi.org/10.1007/s10118-020-2448-0

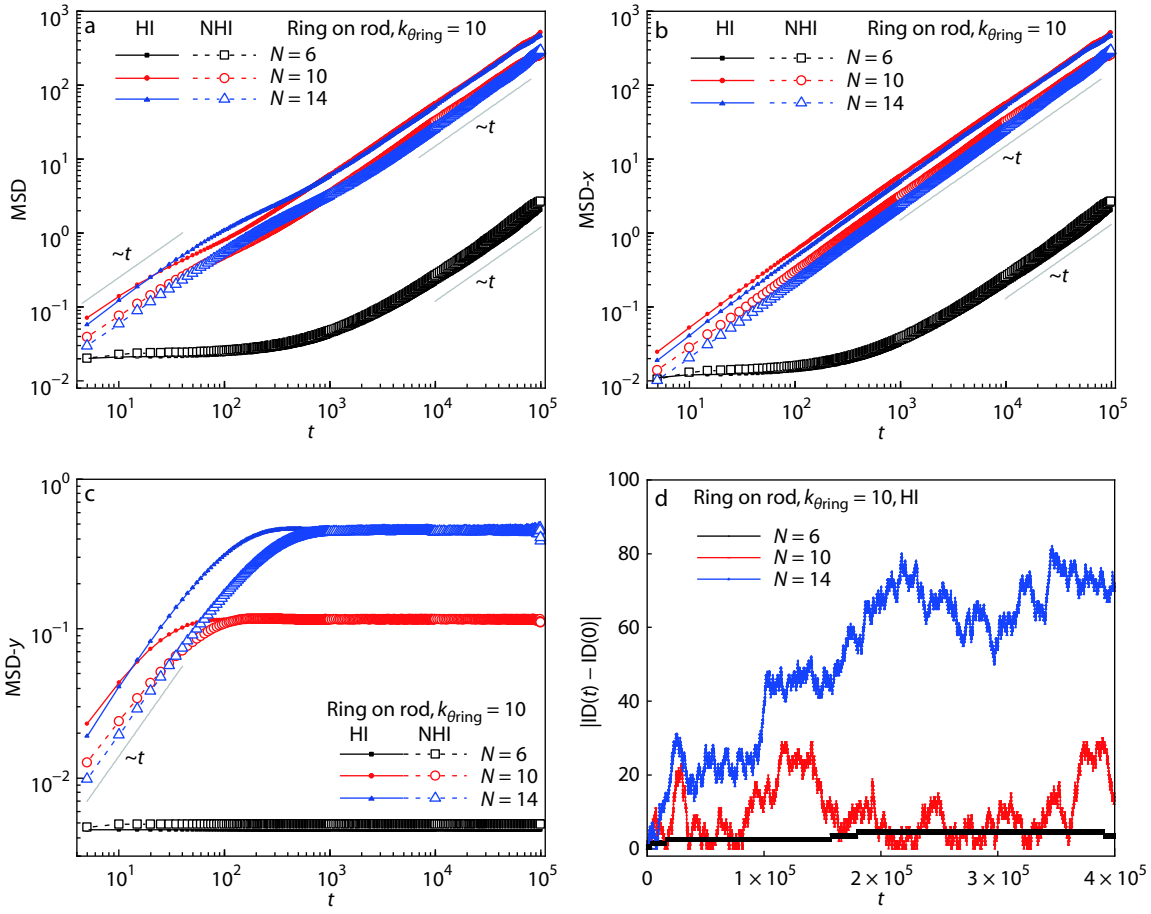

Fig. 3 The center-of-mass mean-square displacement (MSD) of ring polymers on a fixed rod. (a) MSD and corresponding (b) *x*- and (c) *y*-components based on the Cartesian coordinates for ring polymers with different sizes. (d) Sliding motion of ring polymers on a fixed rod with hydrodynamic interactions.

rings, it makes no difference whether hydrodynamic interactions are considered.

As the ring size increases further, the strong interaction between rings and axial chains is greatly reduced, and the MSD of rings is drastically enhanced compared with that for small rings. The corresponding MSD curves exhibit three characteristic regions. In short-time and long-time regions, MSD ~ *t*. In the transition region, MSD ~ t^a ($a < 1$), which is caused by the transition from 3D diffusion at the initial stage to 1D diffusion at long time scale of the threaded ring. In a very short period of time, large rings diffuse freely without being aware of the axial chain at small length scales. As the time increases, the motion of threaded ring is largely restricted by the axial chain, resulting in a sub-diffusion region. At a long-time limit, the ring dynamics can be reduced to one-dimensional diffusion, where the axial diffusion plays a dominant role. We also estimated the sliding motion of threaded rings and the results are presented in Fig. 3(d). As the ring size increases, the reduction of repulsive interactions between rings and axial chains leads to significantly enhanced sliding motions of threaded rings.

The diffusion coefficients based on the Cartesian coordinates for ring polymers with different sizes can be calculated quantitatively by using Eq. (12) at long time scales, as shown in Fig. 4(a). It is clear that the hydrodynamic interactions also speed up the ring diffusion on a fixed axial chain. The diffusion coefficients for both HI and NHI increase at first with the ring size and reach a peak value at $N = 8$, because large rings significantly reduce the interaction between the threaded ring and axial chain. By further increasing the ring size, such interaction becomes negligible, resulting in the decrease of ring mobility. This is consistent with the above discussion that a large ring slows down its diffusion dynamics in free space. The motion of threaded rings can be considered as a one-dimensional diffusion, which means that the relative diffusion D/D_0 for large rings should be 1/3. Our simulation results for NHI show that the relative diffusion D/D_0 approaches a saturation value about 0.37 (Fig. 4b), in agreement with the theoretical prediction. It is worth noting that D/D_0 exhibits a monotonic dependence on the chain length for systems with hydrodynamic interactions being considered, indicating that the ring dynamics is closely related to hydrodynamic interactions.

Threaded Ring on Flexible Chain

The sliding dynamics of rings threaded on a flexible axial chain is investigated as a comparison with the axial rod. Fig. 5(a) shows the center-of-mass mean-square displacement (MSD) for ring polymers with and without hydrodynamic interactions. As

mentioned before, small rings are "attached" to fixed positions on the axial chain. Therefore, MSDs for $N = 6$ result mainly from the conformational fluctuations of the flexible axial chain. Obviously, the absolute diffusion of rings and fluctuation of axial chain are significantly enhanced by the inclusion of hydrodynamic interactions. Given that the flexible axial chain is connected *via* periodic boundary conditions, the *x*-component of MSD at longer times is greater than that of small rings (Fig. 5b NHI), indicating the dominant role of sliding diffusion for large rings is the hydrodynamic interactions.

At short time scales, MSD and its *x*-component for large rings scale linearly with time. Subsequently, the ring dynamics behaves like the super-diffusion mode, MSD ~ t^a, and $a > 1$. In this time scale, the ring itself diffuses along the axial chain, and the axial chain reptates back and forth through the ring. Such two motion modes couple with each other, result-

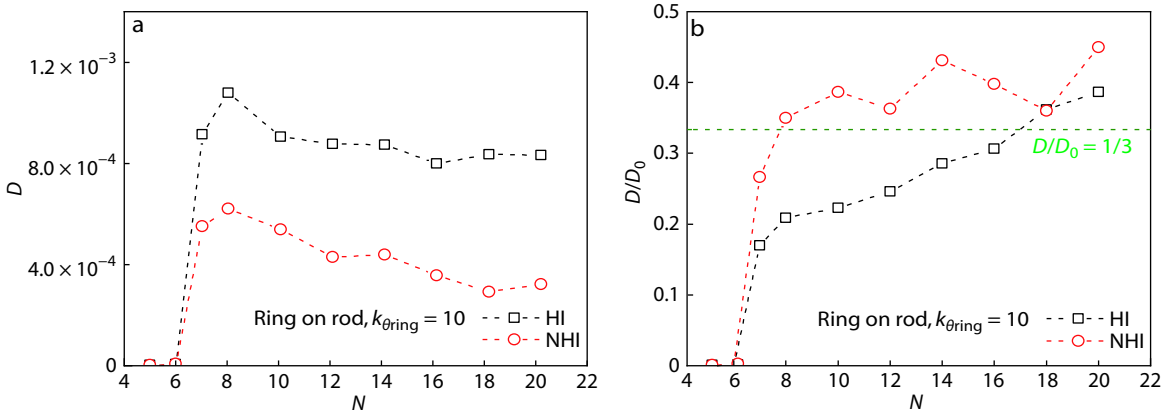

Fig. 4 The diffusion coefficients of ring polymers on a fixed rod with and without hydrodynamic interactions. (a) The diffusion coefficients D and (b) relative diffusion D/D_0 for ring polymers with different sizes.

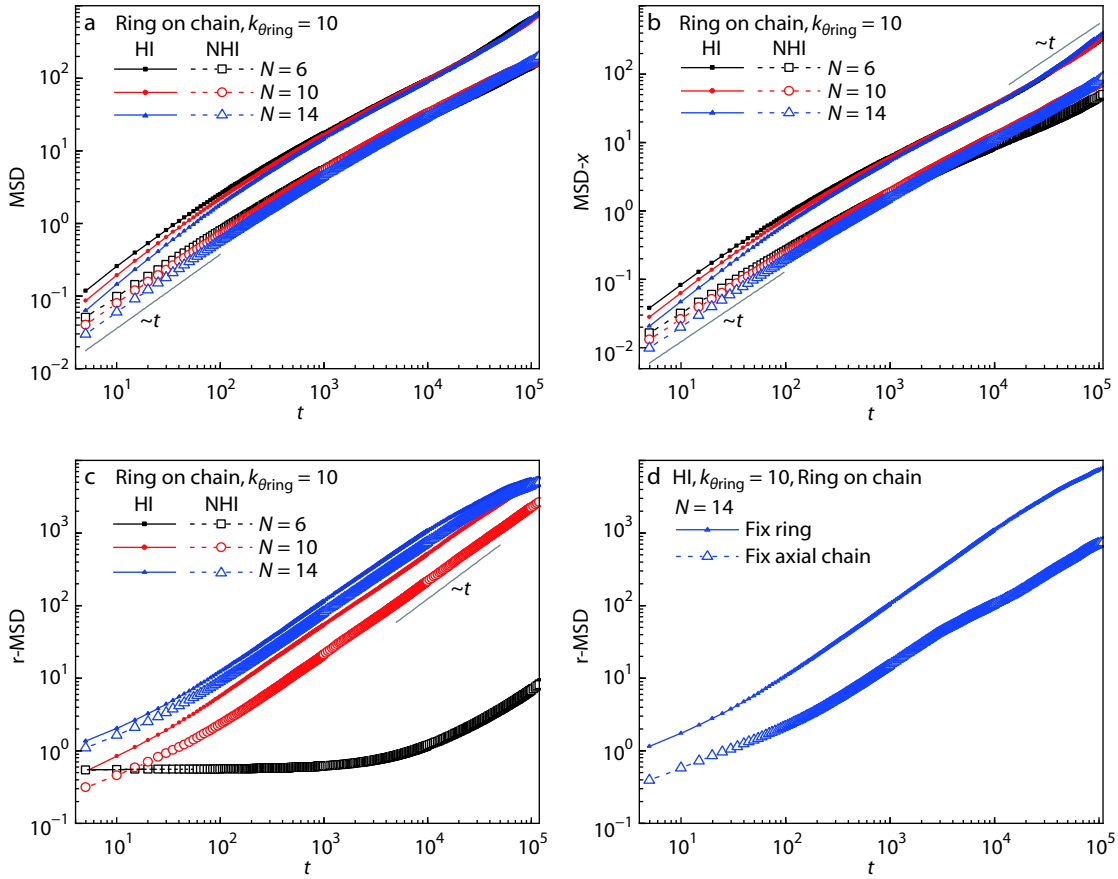

Fig. 5 The center-of-mass mean-square displacement (MSD) of ring polymers on a flexible polymer chain. (a) MSD and corresponding (b) *x*-component based on the Cartesian coordinates for ring polymers with different sizes. (c) Relative MSD of ring polymers on a flexible chain with and without hydrodynamic interactions. (d) Sliding MSD for threaded rings with ring and axial chain being fixed.

https://doi.org/10.1007/s10118-020-2448-0

ing in cooperative movement of the threaded ring. The sliding motion is characterized by r-MSD, as shown in Fig. 5(c). The ring dynamics displays a one-dimensional diffusion at long time scales. In order to analyze the contributions of different components in the threaded-ring structure, we design two different simulation systems with the same initial conformations: (1) fixed ring with free axial chain; (2) free ring with fixed axial chain. A group of representative results for $N = 14$ is given in Fig. 5(d). Here, "Fix ring" corresponds to the reptation motion of axial chain and "Fix axial chain" corresponds to the self-diffusion of ring, respectively. As shown in Fig. 5(d), the reputation-like motion of axial chain plays a dominant role in the relative sliding motion of threaded rings.

The sliding diffusion coefficients for ring polymers with different sizes can be calculated quantitatively by using Eq. (12) at long time scales, as shown in Fig. 6(a). It is clear that the sliding diffusion of rings is significantly enhanced by hydrodynamic interactions for both systems of Ring-on-Rod and Ring-on-Chain. For rings threaded on an axial rod, the diffusion increases at first and then decreases, with the peak value at $N = 8$ (see inset of Fig. 6a). As for rings threaded on the flexible axial chain, the inclusion of hydrodynamic interactions results in a monotonic increase of ring diffusion. Meanwhile, compared with the ideal rod-like chain, the flexible axial chain results in faster sliding motions of threaded rings, implying a weaker entropic barrier. It is worth noting that the entropic barrier plays a crucial role in dictating polymer transportation through narrow channels under external fields. In such situation, the polymer chain is strongly stretched and far from its equilibrium state, while for the threaded ring under equilibrium conditions, the simulation results suggest that the entropic barrier is negligible. Theoretically, the tube theory is the most widely accepted model to characterize the rheological behavior of entangled polymers. In tube theory, the complex many-body effects of molecular interpenetration are simplified as a smooth, tube-like confinement on a test chain. The faster sliding of threaded rings agrees well with the basic assumption of barrier-less confining tube at equilibrium. Moreover, hydrodynamic interactions significantly amplify the speedup effects of flexible axial chain on the ring diffusion.

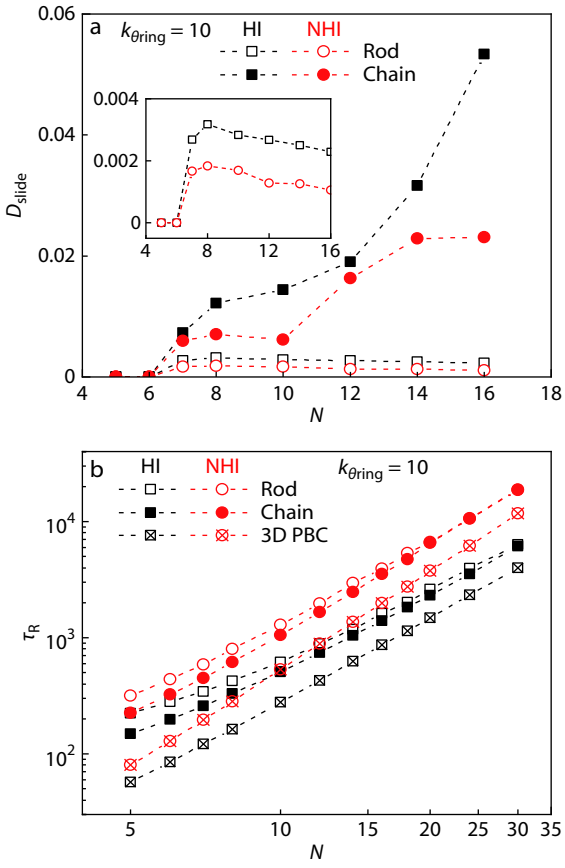

Fig. 6 The (a) sliding diffusion coefficients and (b) relaxation time of ring polymers threaded on rod and flexible chains.

We also calculated the relaxation of rings at three different situations (in free space, threaded on rod, threaded on chain), and the results are given in Fig. 6(b). Similar to the results in free space, hydrodynamic interactions speed up the relaxation dynamics. In addition, small rings threaded on a flexible chain relax faster than that on a rod chain, which results from the cooperative relaxation of ring and axial chains. Such a difference disappears with the ring size. A comparison between the results of Figs. 6(a) and 6(b) indicates that the diffusion and relaxation are decoupled for threaded rings, suggesting the breakdown of the Einstein-Stokes relation.

CONCLUSIONS

We systemically studied the sliding dynamics of rings threaded on different axial polymers and quantitatively evaluated the effects of hydrodynamic interactions by using a hybrid simulation method which combines multi-particle collision dynamics with molecular dynamics. We found that the hydrodynamic interactions significantly speed up the diffusion and relaxation behaviors of free and threaded rings. Moreover, the diffusion motion of ring itself couples with the reptation-like motion of the flexible axial chain, leading to an enhanced cooperative movement of the threaded ring. Both the absolute diffusion and the reptation-like motion are accelerated by taking account of hydrodynamic interactions. Finally, the diffusion and relaxation behaviors for threaded rings are decoupled, indicating the breakdown of the Einstein-Stokes relationship.

Furthermore, the faster sliding dynamics of threaded ring on flexible axial chain in equilibrium implies that the entropy barrier for threaded ring exerted by the axial chain is negligible. Such results agree well with the basic assumption of barrier-less confining tube at equilibrium in tube theory, a widely accepted model in describing the entangled polymer melts. In addition, the conformational behaviors of polymer chain non-monotonically depend on its rigidity, and the semiflexible chain usually possesses stronger conformational entropy.[78,79] Therefore, our future work will focus on the effects of axial chain rigidity on the dynamics and hydrodynamic interactions of threaded rings. And further investigations will be performed to deal with the intrinsic relation between threaded-ring structure and polymer rheology. We hope that our results of this work provide novel insights in understanding the effects of topologies and entanglements on the properties of polymeric fluids.

https://doi.org/10.1007/s10118-020-2448-0

ACKNOWLEDGMENTS

This work was financially supported by the Science Challenge Project (No. TZ2018004), the National Natural Science Foundation of China (Nos. 21790340 and 21674113), Jilin Scientific and Technological Development Program (No. 20180519001JH), and the Programs of Chinese Academy of Sciences (Nos. QYZDY-SSW-SLH027 and YJKYYQ20190084). Y.L. acknowledges the Youth Innovation Promotion Association of Chinese Academy of Sciences (No. 2016204) for financial support.

REFERENCES

1 Doi, M.; Edwards, S. F. *The theory of polymer dynamics*. Oxford University Press, **1988**.
2 Roovers, J. The melt properties of ring polystyrenes. *Macromolecules* **1985**, *18*, 1359–1361.
3 Roovers, J. Viscoelastic properties of polybutadiene rings. *Macromolecules* **1988**, *21*, 1517–1521.
4 McKenna, G. B.; Hostetter, B. J.; Hadjichristidis, N.; Fetters, L. J.; Plazek, D. J. A study of the linear viscoelastic properties of cyclic polystyrenes using creep and recovery measurements. *Macromolecules* **1989**, *22*, 1834–1852.
5 Mills, P. J.; Mayer, J. W.; Kramer, E. J.; Hadziioannou, G.; Lutz, P.; Strazielle, C.; Rempp, P.; Kovacs, A. J. Diffusion of polymer rings in linear polymer matrices. *Macromolecules* **1987**, *20*, 513–518.
6 Iyer, B. V. S.; Lele, A. K.; Shanbhag, S. What is the size of a ring polymer in a ring-linear blend? *Macromolecules* **2007**, *40*, 5995–6000.
7 Subramanian, G.; Shanbhag, S. Self-diffusion in binary blends of cyclic and linear polymers. *Macromolecules* **2008**, *41*, 7239–7242.
8 Yang, Y.; Sun, Z.; Fu, C.; An, L.; Wang, Z. G. Monte Carlo simulation of a single ring among linear chains: structural and dynamic heterogeneity. *J. Chem. Phys.* **2010**, *133*, 064901.
9 Halverson, J. D.; Grest, G. S.; Grosberg, A. Y.; Kremer, K. Rheology of ring polymer melts: from linear contaminants to ring-linear blends. *Phys. Rev. Lett.* **2012**, *108*, 038301.
10 Gooßen, S.; Krutyeva, M.; Sharp, M.; Feoktystov, A.; Allgaier, J.; Pyckhout-Hintzen, W.; Wischnewski, A.; Richter, D. Sensing polymer chain dynamics through ring topology: a neutron spin echo study. *Phys. Rev. Lett.* **2015**, *115*, 148302.
11 Kapnistos, M.; Lang, M.; Vlassopoulos, D.; Pyckhout-Hintzen, W.; Richter, D.; Cho, D.; Chang, T.; Rubinstein, M. Unexpected power-law stress relaxation of entangled ring polymers. *Nat. Mater.* **2008**, *7*, 997–1002.
12 Aoki, D.; Takata, T. Mechanically linked supramolecular polymer architectures derived from macromolecular [2]rotaxanes: synthesis and topology transformation. *Polymer* **2017**, *128*, 276–296.
13 Takata, T.; Aoki, D. Topology-transformable polymers: linear-branched polymer structural transformation *via* the mechanical linking of polymer chains. *Polym. J.* **2018**, *50*, 127–147.
14 Takata, T. Switchable polymer materials controlled by rotaxane macromolecular switches. *ACS Cent. Sci.* **2020**, *6*, 129–143.
15 Metzler, R.; Kantor, Y.; Kardar, M. Force-extension relations for polymers with sliding links. *Phys. Rev. E* **2002**, *66*, 022102.
16 Baulin, V. A.; Johner, A.; Marques, C. M. Sliding grafted polymer layers. *Macromolecules* **2005**, *38*, 1434–1441.
17 Baulin, V. A.; Lee, N. K.; Johner, A.; Marques, C. M. Micellization of sliding polymer surfactants. *Macromolecules* **2006**, *39*, 871–876.
18 Ramírez-Hernández, A.; Detcheverry, F. A.; Peters, B. L.; Chappa, V. C.; Schweizer, K. S.; Müller, M.; de Pablo, J. J. Dynamical simulations of coarse grain polymeric systems: rouse and entangled dynamics. *Macromolecules* **2013**, *46*, 6287–6299.
19 Gustafson, A.; Morse, D. C. A reptation model of slip at entangled polymer-polymer interfaces. *Macromolecules* **2016**, *49*, 7032–7044.
20 Brackley, C. A.; Johnson, J.; Michieletto, D.; Morozov, A. N.; Nicodemi, M.; Cook, P. R.; Marenduzzo, D. Nonequilibrium chromosome looping *via* molecular slip links. *Phys. Rev. Lett.* **2017**, *119*, 138101.
21 Frisch, H. L.; Wasserman, E. Chemical topology. *J. Am. Chem. Soc.* **1961**, *83*, 3789–3795.
22 Schill, G. *Catenanes, rotaxanes, and knots*. Academic Press, New York, **1971**.
23 Sauvage, J. P.; Dietrich-Buchecker, C. *Molecular catanes, rotaxanes and knots: a journey through the world of molecular topology*. Wiely-VCH, Weinheim, **1999**.
24 Fang, L.; Olson, M. A.; Benítez, D.; Tkatchouk, E.; Goddard Iii, W. A.; Stoddart, J. F. Mechanically bonded macromolecules. *Chem. Soc. Rev.* **2010**, *39*, 17–29.
25 Forgan, R. S.; Sauvage, J. P.; Stoddart, J. F. Chemical topology: complex molecular knots, links, and entanglements. *Chem. Rev.* **2011**, *111*, 5434–5464.
26 Sauvage, J. P. From chemical topology to molecular machines (Nobel lecture). *Angew. Chem. Int. Ed.* **2017**, *56*, 11080–11093.
27 Deutman, A. B. C.; Monnereau, C.; Elemans, J. A. A. W.; Ercolani, G.; Nolte, R. J. M.; Rowan, A. E. Mechanism of threading a polymer through a macrocyclic ring. *Science* **2008**, *322*, 1668–1671.
28 Balzani, V.; Gómez-López, M.; Stoddart, J. F. Molecular machines. *Accounts. Chem. Res.* **1998**, *31*, 405–414.
29 van Dongen, S. F. M.; Cantekin, S.; Elemans, J.; Rowan, A. E.; Nolte, R. J. M. Functional interlocked systems. *Chem. Soc. Rev.* **2014**, *43*, 99–122.
30 Erbas-Cakmak, S.; Leigh, D. A.; McTernan, C. T.; Nussbaumer, A. L. Artificial molecular machines. *Chem. Rev.* **2015**, *115*, 10081–10206.
31 Xue, M.; Yang, Y.; Chi, X.; Yan, X.; Huang, F. Development of pseudorotaxanes and rotaxanes: from synthesis to stimuli-responsive motions to applications. *Chem. Rev.* **2015**, *115*, 7398–7501.
32 Yu, G.; Yung, B. C.; Zhou, Z.; Mao, Z.; Chen, X. Artificial molecular machines in nanotheranostics. *ACS Nano* **2018**, *12*, 7–12.
33 Anelli, P. L.; Spencer, N.; Stoddart, J. F. A molecular shuttle. *J. Am. Chem. Soc.* **1991**, *113*, 5131–5133.
34 Zhu, K.; Baggi, G.; Loeb, S. J. Ring-through-ring molecular shuttling in a saturated [3]rotaxane. *Nat. Chem.* **2018**, *10*, 625–630.
35 Corra, S.; de Vet, C.; Groppi, J.; La Rosa, M.; Silvi, S.; Baroncini, M.; Credi, A. Chemical on/off switching of mechanically planar chirality and chiral anion recognition in a [2]rotaxane molecular shuttle. *J. Am. Chem. Soc.* **2019**, *141*, 9129–9133.
36 Bissell, R. A.; Córdova, E.; Kaifer, A. E.; Stoddart, J. F. A chemically and electrochemically switchable molecular shuttle. *Nature* **1994**, *369*, 133–137.
37 Deng, W. Q.; Muller, R. P.; Goddard, W. A. Mechanism of the Stoddart-Heath bistable rotaxane molecular switch. *J. Am. Chem. Soc.* **2004**, *126*, 13562–13563.
38 Lohmann, F.; Ackermann, D.; Famulok, M. Reversible light switch for macrocycle mobility in a DNA rotaxane. *J. Am. Chem. Soc.* **2012**, *134*, 11884–11887.
39 Bruns, C. J.; Stoddart, J. F. Rotaxane-based molecular muscles. *Accounts. Chem. Res.* **2014**, *47*, 2186–2199.
40 de Gennes, P. G. Sliding gels. *Physica A* **1999**, *271*, 231–237.
41 Helfer, C. A.; Xu, G.; Mattice, W. L.; Pugh, C. Monte Carlo simulations investigating the threading of cyclic poly(ethylene oxide) by linear chains in the melt. *Macromolecules* **2003**, *36*, 10071–10078.

42 Urakami, N.; Imada, J.; Yamamoto, T. Simulation of pseudopolyrotaxane formation and orientational order between pseudopolyrotaxanes. *J. Chem. Phys.* **2010**, *132*, 054901.
43 Pinson, M. B.; Sevick, E. M.; Williams, D. R. M. Mobile rings on a polyrotaxane lead to a yield force. *Macromolecules* **2013**, *46*, 4191–4197.
44 Gilles, F. M.; Llubaroff, R.; Pastorino, C. Fluctuation-induced forces between rings threaded around a polymer chain under tension. *Phys. Rev. E* **2016**, *94*, 032503.
45 Müller, T.; Sommer, J. U.; Lang, M. Tendomers-force sensitive bis-rotaxanes with jump-like deformation behavior. *Soft Matter* **2019**, *15*, 3671–3679.
46 Lee, E.; Kim, S.; Jung, Y. Slowing down of ring polymer diffusion caused by inter-ring threading. *Macromol. Rapid Commun.* **2015**, *36*, 1115–1121.
47 Lee, E.; Jung, Y. Slow dynamics of ring polymer melts by asymmetric interaction of threading configuration: Monte Carlo study of a dynamically constrained lattice model. *Polymers* **2019**, *11*, 516.
48 Zhou, Y.; Hsiao, K.-W.; Regan, K. E.; Kong, D.; McKenna, G. B.; Robertson-Anderson, R. M.; Schroeder, C. M. Effect of molecular architecture on ring polymer dynamics in semidilute linear polymer solutions. *Nat. Commun.* **2019**, *10*, 1753.
49 Araki, J.; Ito, K. Recent advances in the preparation of cyclodextrin-based polyrotaxanes and their applications to soft materials. *Soft Matter* **2007**, *3*, 1456–1473.
50 Murata, N.; Konda, A.; Urayama, K.; Takigawa, T.; Kidowaki, M.; Ito, K. Anomaly in stretching-induced swelling of slide-ring gels with movable cross-links. *Macromolecules* **2009**, *42*, 8485–8491.
51 Ito, K. Novel entropic elasticity of polymeric materials: why is slide-ring gel so soft? *Polym. J.* **2012**, *44*, 38–41.
52 Noda, Y.; Hayashi, Y.; Ito, K. From topological gels to slide-ring materials. *J. Appl. Polym. Sci.* **2014**, 131.
53 Ito, K. Novel cross-linking concept of polymer network: synthesis, structure, and properties of slide-ring gels with freely movable junctions. *Polym. J.* **2007**, *39*, 489–499.
54 Okumura, Y.; Ito, K. The polyrotaxane gel: a topological gel by figure-of-eight cross-links. *Adv. Mater.* **2001**, *13*, 485–487.
55 Liu, C.; Kadono, H.; Mayumi, K.; Kato, K.; Yokoyama, H.; Ito, K. Unusual fracture behavior of slide-ring gels with movable cross-links. *ACS Macro Lett.* **2017**, *6*, 1409–1413.
56 Jiang, L.; Liu, C.; Mayumi, K.; Kato, K.; Yokoyama, H.; Ito, K. Highly stretchable and instantly recoverable slide-ring gels consisting of enzymatically synthesized polyrotaxane with low host coverage. *Chem. Mater.* **2018**, *30*, 5013–5019.
57 Yasuda, Y.; Hidaka, Y.; Mayumi, K.; Yamada, T.; Fujimoto, K.; Okazaki, S.; Yokoyama, H.; Ito, K. Molecular dynamics of polyrotaxane in solution investigated by quasi-elastic neutron scattering and molecular dynamics simulation: sliding motion of rings on polymer. *J. Am. Chem. Soc.* **2019**, *141*, 9655–9663.
58 Yasuda, Y.; Toda, M.; Mayumi, K.; Yokoyama, H.; Morita, H.; Ito, K. Sliding dynamics of ring on polymer in rotaxane: a coarse-grained molecular dynamics simulation study. *Macromolecules* **2019**, *52*, 3787–3793.
59 Teraoka, I. *Polymer solutions: an introduction to physical properties*. John Wiley & Sons, Inc., New York, USA, **2002**.
60 Kikuchi, N.; Gent, A.; Yeomans, J. M. Polymer collapse in the presence of hydrodynamic interactions. *Eur. Phys. J. E* **2002**, *9*, 63–66.
61 Kikuchi, N.; Ryder, J. F.; Pooley, C. M.; Yeomans, J. M. Kinetics of the polymer collapse transition: the role of hydrodynamics. *Phys. Rev. E* **2005**, *71*, 061804.
62 Piili, J.; Suhonen, P. M.; Linna, R. P. Uniform description of polymer ejection dynamics from capsid with and without hydrodynamics. *Phys. Rev. E* **2017**, *95*, 052418.
63 Sendner, C.; Netz, R. R. Single flexible and semiflexible polymers at high shear: non-monotonic and non-universal stretching response. *Eur. Phys. J. E* **2009**, *30*, 75.
64 Chan, N. Y.; Chen, M.; Hao, X. T.; Smith, T. A.; Dunstan, D. E. Polymer compression in shear flow. *J. Phys. Chem. Lett.* **2010**, *1*, 1912–1916.
65 Saha Dalal, I.; Hoda, N.; Larson, R. G. Multiple regimes of deformation in shearing flow of isolated polymers. *J. Rheol.* **2012**, *56*, 305–332.
66 Saha Dalal, I.; Albaugh, A.; Hoda, N.; Larson, R. G. Tumbling and deformation of isolated polymer chains in shearing flow. *Macromolecules* **2012**, *45*, 9493–9499.
67 Wang, Z.; Zhai, Q.; Chen, W.; Wang, X.; Lu, Y.; An, L. Mechanism of nonmonotonic increase in polymer size: comparison between linear and ring chains at high shear rates. *Macromolecules* **2019**, *52*, 8144–8154.
68 Malevanets, A.; Kapral, R. Mesoscopic model for solvent dynamics. *J. Chem. Phys.* **1999**, *110*, 8605.
69 Gompper, G.; Ihle, T.; Kroll, D. M.; Winkler, R. G. Multi-particle collision dynamics: a particle-based mesoscale simulation approach to the hydrodynamics of complex fluids. *Advanced Computer Simulation Approaches for Soft Matter Sciences III* **2009**, *221*, 1–87.
70 Ihle, T.; Kroll, D. M. Stochastic rotation dynamics: a Galilean-invariant mesoscopic model for fluid flow. *Phys. Rev. E* **2001**, *63*, 020201.
71 Kremer, K.; Grest, G. S. Dynamics of entangled linear polymer melts: a molecular-dynamics simulation. *J. Chem. Phys.* **1990**, *92*, 5057.
72 Rubinstein, M.; Colby, R. H. *Polymer physics*. Oxford University Press, **2003**.
73 Allen, M. P.; Tildesley, D. J. *Computer simulation of liquids*. Oxford University Press, **1989**.
74 Malevanets, A.; Yeomans, J. M. Dynamics of short polymer chains in solution. *Europhys. Lett.* **2000**, *52*, 231.
75 Nikoubashman, A.; Likos, C. N. Flow-induced polymer translocation through narrow and patterned channels. *J. Chem. Phys.* **2010**, *133*, 074901.
76 Cannavacciuolo, L.; Winkler, R. G.; Gompper, G. Mesoscale simulations of polymer dynamics in microchannel flows. *Europhys. Lett.* **2008**, *83*, 34007.
77 Watari, N.; Makino, M.; Kikuchi, N.; Larson, R. G.; Doi, M. Simulation of DNA motion in a microchannel using stochastic rotation dynamics. *J. Chem. Phys.* **2007**, *126*, 094902.
78 Xu, G.; Huang, Z.; Chen, P.; Cui, T.; Zhang, X.; Miao, B.; Yan, L. T. Optimal reactivity and improved self-healing capability of structurally dynamic polymers grafted on Janus nanoparticles governed by chain stiffness and spatial organization. *Small* **2017**, *13*, 1603155.
79 Yu, Q.; Wang, R. Effect of chain rigidity on the crystallization of DNA-directed nanoparticle system. *Macromolecules* **2018**, *51*, 8372–8376.

https://doi.org/10.1007/s10118-020-2448-0